Inorg. Chem. **2007**, *46*, 6958–6967

Inorganic Chemistry
Article

Coordinatively Unsaturated Semisandwich Complexes of Ruthenium with Phosphinoamine Ligands and Related Species: A Complex Containing (*R*,*R*)-1,2-Bis((diisopropylphosphino)amino)cyclohexane in a New Coordination Form $\kappa^3 P,P',N$-η^2-P,N

M. Dolores Palacios,[†] M. Carmen Puerta,[†] Pedro Valerga,[*,†] Agustí Lledós,[‡] and Edouard Veilly[‡]

Departamento de Ciencia de Materiales e Ingeniería Metalúrgica y Química Inorgánica, Facultad de Ciencias, Universidad de Cádiz, 11510 Puerto Real, Cádiz, Spain, and Departament de Química, Edifici Cn, Universitat Autònoma de Barcelona, 08193 Bellaterra, Barcelona, Spain

Received April 9, 2007

The syntheses of the chloro complexes [Ru(η^5-C_5R_5)Cl(L)] (R = H, Me; L = phosphinoamine ligand) (**1a**–**d**) have been carried out by reaction of [(η^5-C_5H_5)RuCl(PPh_3)$_2$] or {(η^5-C_5Me_5)RuCl}$_4$ with the corresponding phosphinoamine (*R*,*R*)-1,2-bis((diisopropylphosphino)amino)cyclohexane), *R*,*R*-dippach, or 1,2-bis(((diisopropylphosphino)amino)ethane), dippae. The chloride abstraction reactions from these compounds lead to different products depending on the starting chlorocomplex and the reaction conditions. Under argon atmosphere, chloride abstraction from [(η^5-C_5Me_5)-RuCl(*R*,*R*-dippach)] with NaBAr′$_4$ yields the compound [(η^5-C_5Me_5)Ru($\kappa^3 P,P'$-(*R*,*R*)-dippach)][BAr′$_4$] (**2b**) which exhibits a three-membered ring Ru–N–P by a new coordination form of this phosphinoamine. However, under the same conditions the reaction starting from [(η^5-C_5Me_5)RuCl(dippae)] yields the unsaturated 16 electron complex [(η^5-C_5Me_5)Ru(dippae)][BAr′$_4$] (**2d**). The bonding modes of *R*,*R*-dippach and dippae ligands have been analyzed by DFT calculations. The possibility of tridentate P,N,P-coordination of the phosphinoamide ligand to a fragment [(η^5-C_5Me_5)Ru]$^+$ is always present, but only the presence of a cyclohexane unit in the ligand framework converts this bonding mode in a more favorable option than the usual P,P-coordination. Dinitrogen [(η^5-C_5R_5)Ru(N_2)(L)][BAr′$_4$] (**3a**–**d**) and dioxygen complexes [(η^5-C_5H_5)Ru(O_2)(*R*,*R*-dippach)][BPh$_4$] (**4a**) and [(η^5-C_5Me_5)Ru(O_2)(L)][BPh$_4$] (**4b**,**d**) have been prepared by chloride abstraction under dinitrogen or dioxygen atmosphere, respectively. The presence of 16 electron [(η^5-C_5H_5)Ru(*R*,*R*-dippach)]$^+$ species in fluorobenzene solutions of the corresponding dinitrogen or dioxygen complexes in conjunction with the presence of [BAr′$_4$]$^-$ gave in some cases a small fraction of [Ru(η^5-C_5H_5)(η^6-C_6H_5F)][BAr′$_4$] (**5a**), which has been isolated and characterized by X-ray diffraction.

Introduction

Polydentate ligands containing phosphorus and nitrogen atoms have been widely used to obtain chelate complexes in coordination chemistry[1−4] and in relation with homogeneous catalysis.[5−10] In particular bis(phosphino)diamines prepared from enantiopures 1,2-diamines have been used like auxiliary ligands in applications of organometallic catalysis for stereoselective organic transformations, like asymmetric hydrogenation reactions,[11−13] asymmetric hydroboration,[14] Diels−Alder catalysis,[15] etc.

---

[*] To whom correspondence should be addressed. E-mail: pedro.valerga@uca.es. Phone: +34 956 016340. Fax: +34 956 016288.

[†] Universidad de Cádiz.

[‡] Universitat Autònoma de Barcelona.

(1) Abdur-Rashid, K.; Guo, R.; Lough, A. J.; Morris, R. H.; Song, D. *Adv. Synth. Catal.* **2005**, *347*, 571.

(2) Diez, J.; Gamasa, M. P.; Gimeno, J.; Rodriguez, Y.; Garcia-Granda, S. *Eur. J. Inorg. Chem.* **2004**, 2078. Cadierno, V.; Gamasa, M. P.; Gimeno, J. *Eur. J. Inorg. Chem.* **2001**, 571.

(3) Balakrishna, M. S.; Panda, R.; Mague, J. T. *Polyhedron* **2003**, *22*, 587.

(4) Jimenez-Tenorio, M.; Palacios, M. D.; Puerta, M. C.; Valerga, P. *Organometallics* **2005**, *24*, 3088.

(5) Zubiri, M. R. I.; Woollins, J. D. *Comm. Inorg. Chem.* **2003**, *24*, 189.

(6) Alajarin, M.; Lopez-Leonardo, C.; Llamas-Lorente, P. *Top. Curr. Chem.* **2005**, *250*, 77.

(7) Gavrilov, K. N.; Polosukhin, A. I. *Russ. J. Coord. Chem.* **2000**, *26*, 652.

(8) Guiry, P. J.; McCarthy, M.; Lacey, P. M.; Saunders, C. P.; Kelly, S.; Connolly, D. J. *Curr. Org. Chem.* **2000**, *4*, 821.

(9) Agbossou-Niedercorn, F.; Suisse, I. *Coord. Chem. Rev.* **2003**, *242*, 145.

(10) Espinet, P.; Soulantica, K. *Coord. Chem. Rev.* **1999**, *193−195*, 499.

10.1021/ic700674c CCC: $37.00

Scheme 1

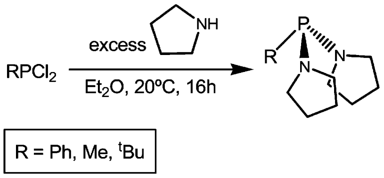

A variety of rhodium,[16−19] palladium,[20] and platinum[21−22] complexes containing these ligands have been synthesized and characterized. Nevertheless, the analogous ruthenium complexes are still scarce, in spite of their increasingly interest during last years.[23−25] Recently, Morris and coworkers have described a series of ruthenium complexes with the diphosphine−diamine system which catalyzes asymmetric hydrogenation reactions of ketones,[26] Michael addition reactions,[27] etc. Chan et al. have reported that palladium complexes containing phosphinoamine are catalysts to the enantioselective allylic alkylation[28] and rhodium complexes are active in catalytic hydrogenation reactions.[29]

The electronic properties of phosphines range from very strong σ-donors alkylphosphines to phosphines with π-acceptor character like the fluoroalkylphosphines. A great variety of species with phosphorus and nitrogen atoms have been described displaying a range of electronic and steric properties. The basicity and the electronic character of the resultant phosphinoamine moieties can be modulated by means of the fragments NR bounded to the phosphorus. For instance, phosphinoamines which were synthesized starting from different chlorophosphines and pyrrolidine (Scheme 1) present even stronger σ-donor character than some trialkylphosphines.[30−33]

Scheme 2

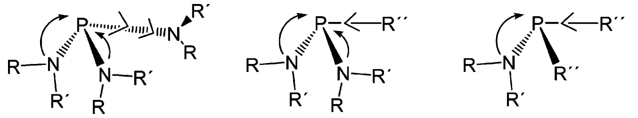

Whereas the donor character and basicity of the phosphinoamine strengthen when only one or two dialkylamine ligands are bonded to the phosphorus, the coordination of three groups $-NR_2$ to the phosphorus causes a decrease in donor properties. X-ray studies of tris(alkylamino)phosphines and complexes containing these ligands show two short bond lengths P−N in the same plane and a third one longer with a nitrogen atom out of the plane. This fact suggested that only two nitrogen atoms can efficiently donate electron pairs to the phosphorus atom, while the last substituent $-NR_2$ acts like an electronegative group decreasing the phosphorus donor properties (Scheme 2).[34]

We have recently reported compounds containing nonchiral dippae (1,2-bis(((diisopropylphosphino)amino)ethane)) or chiral *R*,*R*-dippach phosphinoamine (*R*,*R*-1,2-bis((diisopropylphosphino)amino)cyclohexane) and the ligand hydridotris(pyrazolyl)borate) (Tp) {TpRuCl(L′)} (L′ = *R*,*R*-dippach, dippae).[4] Our study was focussed in the synthesis and characterization of hydride and related compounds and their behavior in protonation reactions with strong and weak acids. This work deals with the study of semisandwich ruthenium systems [Ru(η^5-C$_5$R$_5$)Cl(L)] containing cyclopentadienyl, Cp, or pentamethylcyclopentadienyl, Cp*, and the phosphinoamine ligand *R*,*R*-dippach or dippae in relation with halide abstraction reactions under argon, dinitrogen, or air.

Results and Discussion

The thermal displacement of PPh$_3$ from [(η^5-C$_5$H$_5$)RuCl(PPh$_3$)$_2$] by either *R*,*R*-dippach or dippae in refluxing toluene leads to the corresponding chloro-complexes [(η^5-C$_5$H$_5$)RuCl(*R*,*R*-dippach)] (**1a**) and [(η^5-C$_5$H$_5$)RuCl(dippae)] (**1c**) (Scheme 3). Both **1a**,**c** are obtained as microcrystalline orange solids in high yields. In the ^{1}H NMR spectrum of **1c** the phosphinoamine ligand shows signals corresponding to the methyl groups between 0.8 and 1.5 ppm and two multiplets due to the CH groups at 2.13 and 2.26 ppm. Whereas the proton resonance of NH groups appears at 1.98 ppm, at 4.60 ppm one singlet due to the Cp hydrogens is observed. At temperatures above 213 K one singlet at 118.0 ppm is observed in the ^{31}P{^{1}H} NMR spectrum. However, at 193 K the ethylene chain movement is slow enough to observe two doublets because both phosphorus became nonequivalent. More complex spectra are recorded for **1a** because of the presence of the chiral phosphinoamine ligand.

---

(11) Cucciolito, M. E.; D’Amora, A.; Vitagliano, A. *Organometallics* **2005**, *24*, 3359.
(12) Boaz, N. W.; Ponasik, J. A., Jr.; Large, S. E. *Tetrahedron: Asymmetry* **2005**, *16*, 2063.
(13) Li, X.; Jia, X.; Xu, L.; Kok, S. H. L.; Yip, C. W.; Chan, A. S. C. *Adv. Synth. Catal.* **2005**, *347*, 1904.
(14) Brunel, J.-M.; Buono, G. *Tetrahedron Lett.* **1999**, *40*, 3561.
(15) Carmona, D.; Lahoz, F. J.; Elipe, S.; Oro, L. A.; Lamata, M. P.; Viguri, F.; Sanchez, F.; Martinez, S.; Cativiela, C.; Lopez-Ram, de Viu, M. P. *Organometallics* **2002**, *21*, 5100.
(16) Zhaofu, F.; Thonnessen, H.; Jones, P. G.; Crowe, L.; Harris, R. K.; Schmutzler, R. *Z. Anorg. Allg. Chem.* **2000**, *626*, 1763.
(17) Polosukhin, A. I.; Bondarev, O. G.; Lyubimov, S. E.; Shiryaev, A. A.; Petrovskii, P. V.; Lysenko, K. A.; Gavrilov, K. N. *Russ. J. Coord. Chem.* **2001**, *27*, 591.
(18) Munzenbers, R.; Rademacher, P.; Boese, R. *J. Mol. Struct.* **1998**, *444*, 77.
(19) Powell, J.; May, C. J. *J. Am. Chem. Soc.* **1982**, *104*, 2636.
(20) Zhang, F. Y.; Pai, C. C.; Chan, A. S. C. *J. Am. Chem. Soc.* **1998**, *120*, 5808.
(21) Zijp, E. J.; van der Vlugt, J. I.; Tooke, D. M.; Spek, A. L.; Vogt, D. *Dalton Trans.* **2005**, 512.
(22) Balakrishna, M. S.; Walawalker, M. G. *J. Organomet. Chem.* **2001**, *628*, 76.
(23) Abdur-Rashid, K.; Lough, A. J.; Morris, R. H. *Organometallics* **2001**, *20*, 1047.
(24) Balakrishna, M. S.; Abhyankar, R. M.; Mague, J. T. *J. Chem. Soc., Dalton Trans.* **1999**, 1407.
(25) Faller, J.; W.; Fontaine, P. P. *Organometallics* **2005**, *24*, 4132.
(26) Guo, R.; Lough, A. J.; Morris, R. H.; Song, D. *Organometallics* **2004**, *23*, 5524.
(27) Guo, R.; Morris, R. H.; Song, D. *J. Am. Chem. Soc.* **2005**, *127*, 516.
(28) Chen, X.; Guo, R.; Li, Y.; Chen, G.; Yeung, C. H.; Chan, A. S. C. *Tetrahedron: Asymmetry* **2004**, *15*, 213.
(29) Zhang, F. Y.; Kwok, W. H.; Chan, A. S. C. *Tetrahedron: Asymmetry* **2001**, *12*, 2337.
(30) Rodriguez i Zubiri, M.; Milton, H. L.; Cole-Hamilton, D. J.; Slawin, A. M. Z.; Woollins, J. D. *Inorg. Chem. Commun.* **2004**, *7*, 201.
(31) Clarke, M. L.; Holliday, G. L.; Slawin, A. M. Z.; Woollins, J. D. *J. Chem. Soc., Dalton Trans.* **2002**, 1093.
(32) Clarke, M. L.; Cole-Hamilton, D. J.; Woollins J. D. *J. Chem. Soc., Dalton. Trans*. **2001**, 2721.
(33) Clarke, M. L.; Cole-Hamilton, D. J.; Slawin, A. M. Z.; Woollins, J. D. *Chem. Commun.* **2000**, 2065.
(34) Moloy, K. G.; Petersen, J. L. *J. Am. Chem. Soc.* **1995**, *117*, 7696.

Scheme 3

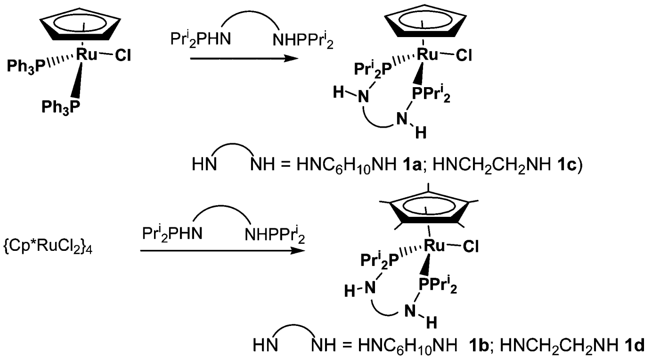

In this case the phosphorus atoms are nonequivalent even at room temperature and the $^{31}P\{^{1}H\}$ NMR spectrum shows two doublets at 112.6 and 113.8 ppm with one coupling constant of 51 Hz. Furthermore, a higher number of signals in the ^{1}H and $^{13}C\{^{1}H\}$ NMR spectra is observed in relation with those of compound **1c**.

The method used to obtain the Cp* analogous has been the reaction between $\{(\eta^5\text{-}C_5Me_5)RuCl\}_4$ and *R*,*R*-dippach or dippae in petroleum ether, yielding the complexes $[(\eta^5\text{-}C_5Me_5)RuCl(R,R\text{-dippach})]$ (**1b**) and $[(\eta^5\text{-}C_5Me_5)RuCl(\text{dippae})]$ (**1d**). ^{1}H NMR spectra of both complexes are similar to those previously discussed of compounds **1a**,**c** except by the presence of $-CH_3$ groups. In the same way, one singlet for **1d** and two doublets for **1c** have been observed in the corresponding $^{31}P\{^{1}H\}$ NMR spectra.

Chloride Abstraction under Argon Atmosphere. In an effort to obtain 16 electron species or the substitution by dinitrogen or dioxygen molecules chloride abstraction reactions under different conditions have been investigated. Under argon we expected the formation of unsaturated complexes. However, the chloride abstraction from the compounds **1b**,**d** under argon with $NaBAr'_4$ leads to very different products. In the case of **1b**, instead of a deep colored material, an orange solution was obtained. A first crop of orange microcrystals needed to be recrystallized affording suitable crystals for X-ray diffraction analysis. An ORTEP view of the cation $[(\eta^5\text{-}C_5Me_5)Ru\ (R,R\text{-dippach})]^+$ in **2b** is shown in Figure 1. The chelation of the diphosphine ligand is reinforced by means of a novel $\kappa^3P,P',N\text{-}\eta^2\text{-}P,N$ coordination in which an amine nitrogen is bounded to the metal in addition to the two phosphorus. A relative stabilization is reached upon the formation of two chelate rings, namely one three-membered and other six-membered metallacycles. We have found in the literature only a related structure for the cobalt complex $[Co\{\kappa^3P,P',N\text{-}(Ph_2PNP(Ph)_2NPPh_2\}\{\kappa^2P,P'\text{-}(Ph_2PNP(Ph)_2NPPh_2\}]$ described by Ellermann et al.[35] But in that case the nitrogen linked to the cobalt has a clear iminic character.

One side of the *R*,*R*-dippach ligand adopts a $\eta^2\text{-}P,N$ coordination with angle P(2)−Ru(1)−N(2) of 44.93(8)° and angles Ru(1)−P(2)−N(2) and Ru(1)−N(2)−P(2) of 66.97(14) and 68.09(12)°, respectively. As expected the bond distance Ru(1)−N(2) of 2.260(4) Å is slightly longer than the values observed for the complex $[(\eta^5\text{-}C_5Me_5)Ru(Me_2NCH_2CH_2NMe_2)]^+$ (2.180(6) and 2.183(7) Å),[36] although closer to the values 2.235(5) and 2.262(5) Å, reported for the complex $[(\eta^5\text{-}C_5Me_5)Ru(Me_2NCH_2CH_2NMe_2)(N{\equiv}CCH_3)]^+$.[37] The Ru−P bond distances on both sides of the ligand Ru(1)−P(2) display a slightly shorter value, 2.2780(12) Å, than for Ru(1)−P(1), 2.3211(12) Å. The additional electronic donation to the metal from nitrogen enhances the basicity on the metal center increasing the back-donation over the phosphorus atom in the three-ring metallacycle. This fact strenghts the bond Ru(1)−P(2) in relation to Ru(1)−P(1) and consequently elongates the bond distance P(2)−N(2) to 1.734(3) Å, in comparison with the value of 1.696(4) Å for P(1)−N(1). Steric effects derived from the trigonal Ru−P−N geometry contribute to fix the limits of values for this set of angles and distances.

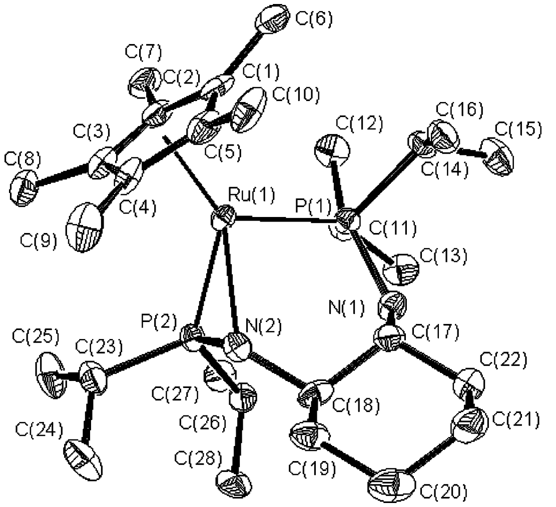

Figure 1. ORTEP drawing (50% thermal ellipsoids) of the cation $[(\eta^5\text{-}C_5Me_5)Ru(R,R\text{-dippach})]^+$ in **2b**. Hydrogen atoms have been omitted. Selected bond lengths (Å) and angles (deg) with estimated standard deviations in parentheses: Ru(1)−P(1), 2.3211(12); Ru(1)−P(2), 2.2780(12); Ru(1)−N(2), 2.260(4); P(2)−N(2), 1.734(3); P(1)−N(1), 1.696(4); P(2)−C(23), 1.856(5); P(1)−C(26), 1.840(4); N(1)−C(17), 1.467(5); N(2)−C(18), 1.518(5); P(1)−Ru(1)−P(2), 93.19(5); P(1)−Ru(1)−N(2), 90.46(9); P(2)−Ru(1)−N(2), 44.93(8); Ru(1)−P(2)−N(2), 66.97(14); Ru(1)−N(2)−P(2), 68.09(12); Ru(1)−P(1)−N(1), 108.85(13); P(2)−N(2)−C(18), 126.2(3); Ru(1)−N(2)−C(18), 128.7(3); Ru(1)−N(2)−H(2), 114(2).

The NMR spectra of **2b** at different temperatures are consistent with the described structure. At room temperature, the ^{1}H NMR spectrum shows one broad signal to Cp* protons while in the $^{31}P\{^{1}H\}$ spectrum a broad singlet appears at 84 ppm. At lower temperatures (210−190 K), the $^{31}P\{^{1}H\}$ NMR resonance decoaleces to two doublets at 71 and 95 ppm (Figure 2). The difference between both chemical shifts agrees with the significative differences in Ru−P bonding. However, a dynamic process renders the phosphorus atoms equivalents at room temperature. This process can be described as an equilibrium through the intermediate 16 electron complex, and it involves alternative breaking and formation of Ru−N bonds (Scheme 4). NMR line-shape

---

(35) Ellermann, J.; Sutter, J.; Knoch, F. A.; Moll, M. *Angew. Chem., Int. Ed. Engl.* **1993**, *32*, 700.

(36) Gemel, C.; Mereiter, K.; Schmid, R.; Kirchner, K. *Organometallics* **1997**, *16*, 5601.

(37) Gemel, C.; LaPensee, A.; Mauthner, K.; Mereiter, K.; Schmid, R.; Kirchner, K. *Monatsh. Chem.* **1997**, *128*, 1189.

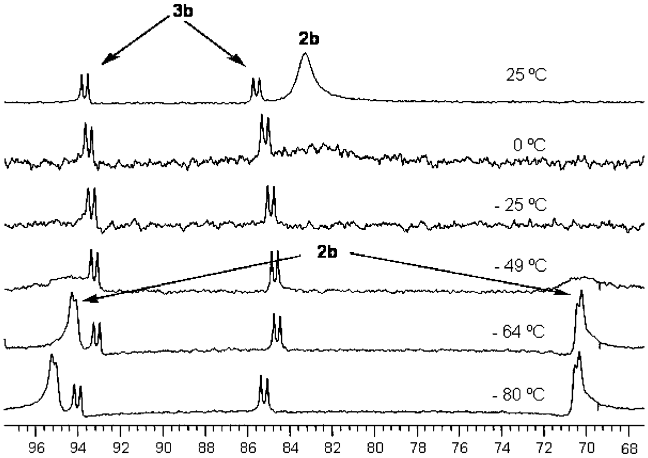

Figure 2. VT $^{31}P\{1H\}$ NMR spectra (161.89 MHz) in CD_2Cl_2 of **2b**.

Scheme 4

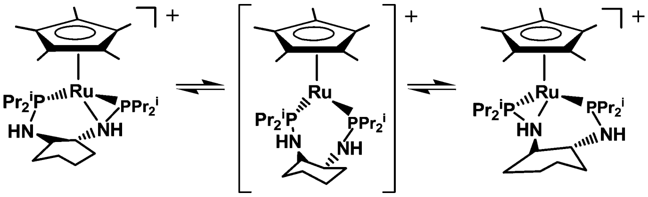

fitting allows the estimation of a value of 8.4(±0.2) kcal·mol^{-1} for the free enthalpy of activation, $\Delta H^{\ddagger}$, and −9(±0.9) cal·mol^{-1}·K^{-1} for the entropy of activation, $\Delta S^{\ddagger}$. On the contrary, ^{1}H NMR spectra using the N−*H* signal did not allow a similar study. N−*H* resonances appear nearest to those corresponding to isopropyl and cyclohexyl C−*H*. All these signals broaden and slightly shift at lower temperatures.

The solutions of **2b** were contaminated by the presence of small amounts of dinitrogen complex $[(\eta^5\text{-}C_5Me_5)Ru(N_2)\text{-}(R,R\text{-dippach})]^+$. Even using a higher purity argon and greatest care in doing the experiments, it was detected in the $^{31}P\{^{1}H\}$NMR spectra at all measured temperatures by two doublets signals at 85 and 94 ppm. In a posterior part of this work, the compound **3b**, containing the dinitrogen complex cation, will be discussed.

Contrary to **1b**, the treatment of $[(\eta^5\text{-}C_5Me_5)RuCl(\text{dippae})]$ (**1d**) with $NaBAr'_4$ allows the isolation of a blue crystalline 16 electron compound $[(\eta^5\text{-}C_5Me_5)Ru(\text{dippae})][BAr'_4]$ (**2d**). We have studied by X-ray crystallography different crystals from samples independently obtained. In all the cases the analyses of data collections allows finding a structure that reveals basically an unsaturated 16 electron skeleton for the cation. Unfortunately, crystal quality, some positional disorder, and other factors did not allow a refinement good enough to be published. Nevertheless, the 16 electron nature of this complex has been confirmed by NMR spectroscopy. In the $^{13}C\{^{1}H)$ NMR spectrum the quaternary Cp* carbons displays a resonance at 66.3 ppm in agreement with other 16 electron cationic complexes of ruthenium, Cp*RuL$_n$.[38−39] We do not discard the presence of a small proportion of a complex with N−Ru interaction as in the case of **2b** already discussed. Studies by VT $^{31P}\{^{1}H\}$ NMR spectroscopy show a singlet at 96.4 ppm at room temperature. At lower temperatures this resonance broadens and gradually coalesces. In the range 213−193 K no signal has been observed in this region. The resonance decoalescence has not been observed even at the lowest temperature. The fluxional process changing chelate ring conformation is very fast. In the case of this unsaturated complex containing dippae with a flexible ethylene chain, temperatures lower than 193 K would be necessary to reduce movement and to observe two nonequivalent phosphorus atoms.

Computational Study of the Bonding Modes of *R*,*R*-dippach and dippae Ligands. One striking feature of the complexes obtained by chloride abstraction under argon atmosphere from $[(\eta^5\text{-}C_5Me_5)RuClL]$ (L = phospinoamine ligand) is the very different bonding mode adopted by the phospinoamine ligand in **2b** (L = (*R*,*R*)-dippach) and **2d** (L = dippae). We have performed a computational study to understand this behavior and to gain an insight into the bonding properties of phospinoamine ligands. The first point analyzed has been to check if both the usual bidentate P,P coordination and the unprecedented tridentate P,N,P are possible with both ligands. To this aim the structure of the **2b**,**d** complexes have been fully optimized with either P,P (**2b-PP**, **2c-PP**) and P,N,P (**2b-PNP**, **2c-PNP**) coordination of the phosphinoamine ligand. Both minima have been found for the two complexes. However the relative stability of both minima is very different depending on the phosphinoamine ligand. With the dippae ligand the 16 electron isomer entailing the usual P,P coordination is found 7.1 kcal·mol^{-1} more stable than the tridentate one. On the contrary, with the *R*,*R*-dippach ligand the 18 electron isomer involving the two chelate rings lies 12.2 kcal·mol^{-1} below the unsaturated one. We have also checked the possibility of a high-spin state for the 16 electron complexes. The singlet state is favored for both ligands, with a very similar singlet−triplet gap (10.1 and 10.2 kcal·mol^{-1} for the *R*,*R*-dippach and dippae complexes, respectively). The computed stabilities fully agree with the experimental characterization of **2b**,**c** as tridentate 18 electron compound and bidentate diamagnetic 16 electron compound, respectively.

We have also checked the possible existence of the P,P- and P,N,P-coordinated minima with a $[(\eta^5\text{-}C_5H_5)Ru]^+$ metal fragment. Indeed both minima are also found for both dippae and *R*,*R*-dippach ligands, proving that the possibility of a tridentate P,N,P coordination, with formation of two chelate rings, also exists with the amino ethane ligand. This alternative could be always present with the phosphinoamine ligands when coordinated to highly unsaturated metal fragments. The energy ordering of the P,P- and P,N,P-coordinated isomers of $[(\eta^5\text{-}C_5H_5)RuL]^+$ complexes is very similar to that found for those of the $[(\eta^5\text{-}C_5Me_5)RuL]^+$ compounds. With the Cp ligand the 16-electron bidentate complex is found 5.4 kcal·mol^{-1} more stable than the

---

(38) Halikhedkar, A.; Jiménez-Tenorio, M.; Puerta, M. C.; Valerga, P.; Sapunov, V. N.; Schmid, R.; Kirchner, K.; Mereiter, K. *Organometallics* **2002**, *21*, 5334.

(39) Gemel, C.; Mereiter, K.; Schmid, R.; Kirchner, K. *Organometallics* **1997**, *16*, 5601.

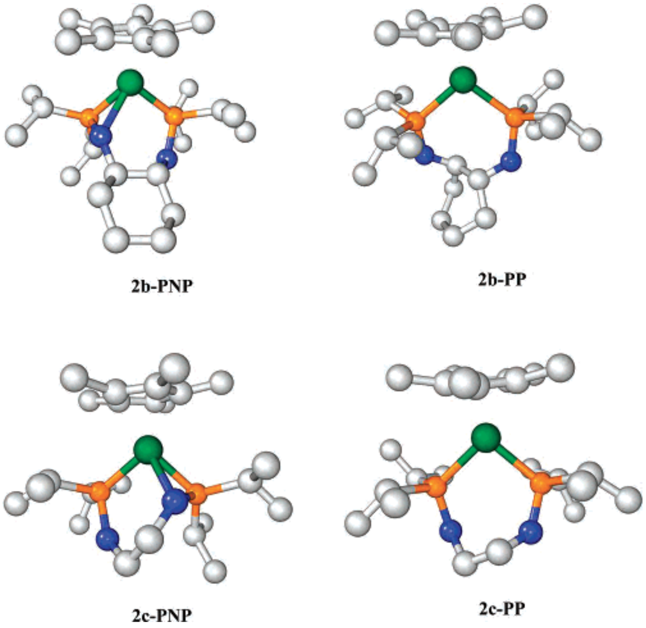

Figure 3. Optimized structures of the P,N,P-coordinated (left) and P,P-coordinated (right) isomers of $[(\eta^5\text{-C}_5\text{Me}_5)\text{Ru}(R,R\text{-dippach})]^+$ (**2b**) and $[(\eta^5\text{-C}_5\text{Me}_5)\text{Ru}(\text{dippae})]^+$ (**2c**). Hydrogen atoms have been omitted for clarity.

Table 1. Selected Geometrical Parameters (Å and deg) of the Optimized Structures of the P,N,P- and P,P-Coordinated Isomers of **2b**,**c**[a]

	$[(\eta^5\text{-C}_5\text{Me}_5)\text{Ru}(R,R\text{-dippach})]^+$		$[(\eta^5\text{-C}_5\text{Me}_5)\text{Ru}(\text{dippae})]^+$	
param	P,N,P	P,P	P,N,P	P,P
Ru−P1	2.403	2.528	2.393	2.518
Ru−P2	2.369	2.510	2.350	2.479
Ru−N2	2.634	3.702	2.304	3.585
P2−N2	1.787	1.719	1.796	1.714
P1−N1	1.742	1.727	1.729	1.739
N1−C17	1.479	1.461	1.465	1.466
N2−C18	1.497	1.464	1.484	1.458
C17−C18	1.537	1.574	1.527	1.526
P1−Ru−P2	93.0	101.8	95.6	96.7
P1−Ru−N2	88.5	79.5	86.2	72.4
P2−Ru−N2	44.4	23.5	45.4	25.3
Ru−P2−N2	67.7	121.0	65.9	116.4
Ru−N2−P2	67.9	35.3	68.7	38.4
Ru−P1−N1	108.1	120.5	114.6	118.5
P2−N2−C18	126.6	123.9	132.1	123.2
Ru−N2−C18	130.5	88.6	124.3	90.1

[a] For the atom numbering, see Figure 1 and Scheme 5.

tridentate 18 electron isomer for L = dippae. On the contrary with L = *R*,*R*-dippach the 18 electron isomer with two chelate rings is found 14.0 kcal·mol^{-1} below the unsaturated one. Clearly the stability of the 16 and 18 electron isomers is governed by the nature of the phosphinoamine ligand.

The optimized geometries of the P,P and P,N,P isomers of $[(\eta^5\text{-C}_5\text{Me}_5)\text{Ru}(R,R\text{-dippach})]^+$ and $[(\eta^5\text{-C}_5\text{Me}_5)\text{Ru}(\text{dippae})]^+$ are depicted in Figure 3. Selected geometrical parameters are collected in Table 1. In a comparison of the optimized structure of **2b-PNP** with the X-ray characterized of **2b** (Figure 1), a good agreement can be observed. From the data in Table 1 it can be appreciated that in addition to the expected shortening of the Ru−N2 distance changing from the P,P to the P,N,P coordination involves remarkable variations in other distances of the chelating ring. These changes are schematized in Scheme 5. The Ru−P bonds are considerably shortened, with the bond distance corresponding to the phosphorus atom participating in the three-member ring (P2) being the shortest one. Furthermore a notable difference is introduced in the two sets of P−N and N−C bond distances depending on the participation of the N in the three-member ring: distances involving the nitrogen atom in the short ring (N2) are longer than those of N1.

Scheme 5. Structural Changes in Passing from the P,P to the P,N,P Coordination[a]

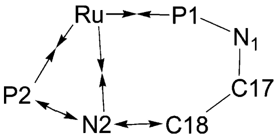

[a] Arrows indicate lengthening (←—→) or shortening (→←) of the bond.

These changes can be explained taking into account the participation of the N lone pair in the Ru−N bond of the P,N,P isomers. In the P,P isomer the N lone pair is partially delocalized in a P═N bond, but it can no longer be delocalized when coordinated to the ruthenium. Accordingly the P−N distance lengthens from 1.719 Å in **2b-PP** to 1.787 Å in **2b-PNP**. A similar change is found in the **2c** isomers.

Another structural feature to be pointed out in the *R*,*R*-dippach complexes is the different conformation adopted by the cyclohexane in the P,P and P,N,P coordination modes, which is apparent in Figure 3. The X-ray structure of **2b** shows a chair cyclohexane conformation. This is also the most stable conformation for the P,N,P coordination found in the computational study. We have also optimized a **2b-PNP** structure with a twist-boat cyclohexane conformation, but it lies 13.9 kcal·mol^{-1} above that with the chair conformation. On the contrary in the structure with the P,P coordination the cyclohexane adopts a twist-boat conformation. Indeed with a twist-boat conformation of cyclohexane the isomer with P,P-coordinated (*R*,*R*-dippach) is 1.7 kcal·mol^{-1} more stable than the P,N,P one. We have also tried to obtain a 16 electron compound with the chair cyclohexane conformation, but all the attempts ended up with a P,N,P coordination of the *R*,*R*-dippach ligand. In this ligand the chair conformation places a nitrogen atom in the vicinity of the unsaturated ruthenium atom, facilitating its coordination to fulfill the 18-electron configuration. This is not the case when the cyclohexane has a twist-boat conformation which places the two nitrogen atom about 3.7 Å far from the metal. The change on the *R*,*R*-dippach from the P,N,P to the P,P coordination mode should imply a conformational change on the cyclohexane unit of the ligand from the most stable chair conformation to the less stable twist-boat one. This factor would enhance the stability of the P,N,P coordination to the $[(\eta^5\text{-C}_5\text{Me}_5)\text{Ru}]^+$ fragment.

To go further in the comparison of the bonding properties of the *R*,*R*-dippach and dippae ligands, we have performed an energy analysis of the transition metal−phosphinoamine coordination using a theoretical approach that we have already employed for investigating the coordination modes of multidentate ligands.[40,41] In this approach we consider the

---

(40) Lledós, A.; Carbó, J.; Navarro, R.; Urriolabeitia, E. P. *Inorg. Chim. Acta* **2004**, *357*, 1444.

Table 2. Energy Decomposition (kcal·mol^{-1}) for the Bonding of Phosphinoamine Ligands to $[(\eta^5\text{-}C_5Me_5)Ru]^+$

	$[[(\eta^5\text{-}C_5Me_5)Ru(R,R\text{-dippach})]^+$		$[[(\eta^5\text{-}C_5Me_5)Ru(dippae)]^+$	
param	P,N,P	P,P	P,N,P	P,P
$\Delta E_{\text{distortion}}$	16.4	10.7	40.5	15.5
$\Delta E_{\text{interaction}}$	−101.8	−83.9	−104.1	−86.2
$\Delta E_{\text{bondingL}}$	−85.4	−73.2	−63.6	−70.1

formation of $[(\eta^5\text{-}C_5Me_5)RuL]^+$ (L = *R*,*R*-dippach, dippae) in the two coordination modes from the $[(\eta^5\text{-}C_5Me_5)Ru]^+$ fragment and the free L ligand. The ΔE value of this reaction is the bonding energy of the phosphinoamine ligand to the $[(\eta^5\text{-}C_5Me_5)RuL]^+$ fragment ($\Delta E_{\text{bondingL}}$). This ΔE can be decomposed into two terms: one accounting for the distortion of L from its isolated optimized geometry to the final geometry in the complex ($\Delta E_{\text{distortion}}$); the other one for the interaction of the distorted complex with the metal fragment to give the complex ($\Delta E_{\text{interaction}}$). The energy values arising from this energy decomposition are gathered in Table 2.

The decomposition of the bonding energy for the two ligands in the two coordination modes clearly shows the factors determining the experimental behavior of *R*,*R*-dippach and dippae with the $[(\eta^5\text{-}C_5Me_5)Ru]^+$ fragment. The interaction energies are very similar for both ligands, the bonding of the N lone pair to the metal always entailing an energy gain of about 18 kcal·mol^{-1}. On the contrary, the distortion terms are very different. Changing from the P,P coordination to the P,N,P one implies a weak distortion of the *R*,*R*-dippach ligand (5.7 kcal·mol^{-1}) but a severe distortion of the dippae one (25 kcal·mol^{-1}). For *R*,*R*-dippach the interaction component compensates the destabilization introduced by the ligand distortion, favoring a tridentate, 18-electron structure. This is not the case with dippae, the greater distortion energy preventing the adoption of the P,N,P coordination. Clearly the presence in the backbone of the phosphinoamine ligand of a cyclohexane makes the complex much more suitable to attain an 18-electron configuration by means of an additional Ru−N bond with only a slight distortion. The cyclohexane part of the *R*,*R*-dippach ligand allows diminishing the distortion energy mainly for the tridentate coordination. The chair conformation of the cyclohexane lays out one of the two nitrogen atoms well disposed to interact with the ruthenium atom.

The last point addressed in the computational study has been the influence of the phospine substituents on the relative stabilities of the 16 and 18 electrons structures. We have optimized the structures of the P,N,P- and P,P-coordinated isomers of $[Cp^*Ru(R,R\text{-dRpach})]^+$ and $[Cp^*Ru(dRpae)]^+$ complexes, with R = H, Me, and Et. The relative energies of the 18 electron tridentate isomers with respect the corresponding 16 electrons bidentate ones are given in Table 3.

Table 3. Relative Energies (kcal·mol^{-1}) of the P,N,P Isomers of $[(\eta^5\text{-}C_5Me_5)Ru(R,R\text{-dRpach})]^+$ and $[(\eta^5\text{-}C_5Me_5)Ru(dRpae)]^+$ Complexes (R = H, Me, Et, ^{i}Pr)[a]

R	$[[(\eta^5\text{-}C_5Me_5)Ru(R,R\text{-dRpach})]^+$	$[(\eta^5\text{-}C_5Me_5)Ru(dRpae)]^+$
H	−6.9	+1.9
Me	−8.5	+5.5
Et	−10.8	+6.1
iPr	−12.2	+7.1

[a] The energy of the corresponding P,P-coordinated isomer has been taken as a zero.

Values in Table 3 show that the change on the phosphine substituents does not modify the energy ordering of both isomers. The P,N,P-coordinated structure is always found more stable than the P,P-one with phosphinoamine cyclohexane ligands (L = dRpach), whatever the R substituents in the phosphine. The contrary happens with phosphinoamine ethane ligands (L = dRpae). However, the energy difference between the 16 and 18 electron compounds is considerably affected by the phosphine substituents. The stability trend is opposite depending on the presence of the ethane or the cyclohexane unit on the ligand framework. With ethane (dRpae ligands) the stability of the 16 electron compound increases in the order H < Me < Et < ^{i}Pr. The effect is particularly important when passing from R = H to R = Me. This is the expected behavior in the stability of unsaturated complexes when increasing the donating capability of the phosphine ligand. On the contrary, phospine substitution in the cyclohexane complexes (dRpach ligands) causes an increased stabilization of the P,N,P isomers. Steric effects and the distortion component of the bonding are responsible for this trend. The phosphinoamine ligands with a cyclohexane are much more suitable for adapting the chain to the constraints imposed by the P,N,P coordination. This is reflected in the values of the PRuP angles in both isomers. Whereas this angle increases notably in the P,P-coordinated structures of $[(\eta^5\text{-}C_5Me_5)Ru(R,R\text{-dRpach})]^+$ complexes (R = H, 86.5°; R = Me = 90.4°; R = Et, 94.1°; R = ^{i}Pr, 101.8°), it only increases 4° in the P,N,P ones (R = H, 88.6°; R = Me, 91.2°; R = Et, 91.8°; R = ^{i}Pr, 93.0°)

Chloride Abstraction under Dinitrogen Atmosphere. When compounds **1a**−**d** are treated by a similar procedure with NaBAr′$_4$ under dinitrogen, they yield the corresponding products $[(\eta^5\text{-}C_5R_5)Ru(N_2)(L)][BAr'_4]$ (**3a**−**d**). The IR spectra of these dinitrogen complexes show the characteristic strong ν(N−N) peak at frequency ranging from 2142 cm^{-1} for **3b** to 2201 cm^{-1} for **3d**. In the $^{31}P\{^1H\}$ NMR spectra of the *R*,*R*-dippach derivatives, two doublets at 110.6 and 112.5 ppm (for **3a**) or at 99.7 and 102.0 ppm (for **3b**) are consistent with the nonequivalence of the two phosphorus. Contrary, in the case of dippae derivatives **3c**,**d** only a singlet appears at room temperature. In a similar way also ^{1}H and $^{31}C\{1H\}$ spectra are more complex in the case of **3a** or **3b**, containing *R*,*R*-dippach, than in the case of **3c** or **3d**.

The X-ray crystal structure of $[(\eta^5\text{-}C_5H_5)Ru(N_2)(R,R\text{-dippach})][BAr'_4]$ (**3a**) has been obtained, and a cation complex drawing is presented in Figure 4. The "three-legged piano stool" structure containing a end-on bounded dinitrogen ligand closely resembles that of the related complex cation $[(\eta^5\text{-}C_5H_5)Ru(N_2)(dippe)]^+$.[42] The distances Ru(1)−N(1) and Ru(2)−N(5) are 1.959(5) and 1.913(6) Å, similar to that

---

(41) Falvelo, L. R.; Ginés, J. C.; Carbó, J.; Lledós, A.; Navarro, R.; Soler, T.; Urriolabeitia, E. P. *Inorg. Chem.* **2006**, *45*, 6803.

(42) Halikhedkar, A.; Jiménez-Tenorio, M.; Puerta, M. C.; Valerga, P.; Mereiter, K. *Organometallics* **2002**, *21*, 628.

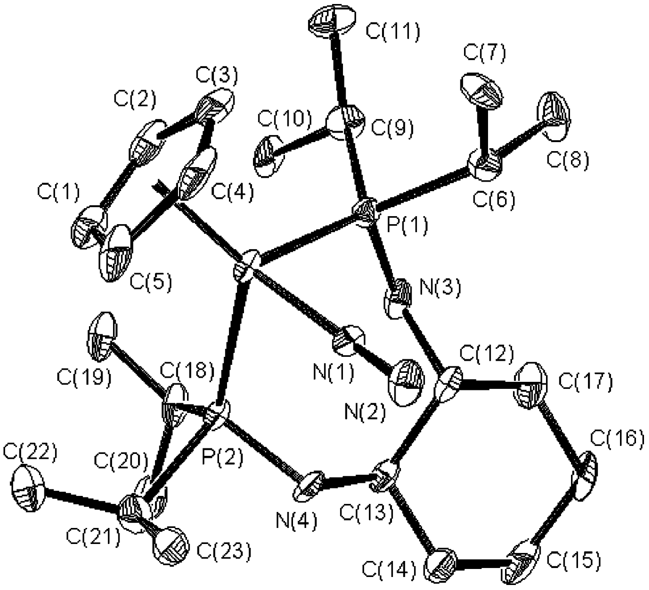

Figure 4. ORTEP drawing (50% thermal ellipsoids) of one complex cation $[(\eta^5\text{-}C_5Me_5)Ru(N_2)(R,R\text{-dippach})]^+$ in **3a**. Hydrogen atoms have been omitted. Selected bond lengths (Å) and angles (deg) with estimated standard deviations in parentheses follow. Cation 1: Ru(1)−P(1), 2.2448(17); Ru(1)−P(2), 2.4148(17); Ru(1)−N(1), 1.959(5); N(1)−N(2), 1.096(7); P(1)−N(3), 1.678(5); P(2)−N(4), 1.614(5); P(1)−Ru(1)−P(2), 95.02(6); P(1)−Ru(1)−N(1), 91.90(15); P(2)−Ru(1)−N(1), 90.83(15); Ru(1)−N(1)−N(2), 175.2(5). Cation 2: Ru(2)−P(3), 2.4142(19); Ru(2)−P(4), 2.2812(18); Ru(2)−N(5), 1.912(6); N(5)−N(6), 1.074(9); P(3)−N(7), 1.595(5); P(4)−N(8), 1.616(5); P(3)−Ru(2)−P(4), 92.21(7); P(3)−Ru(2)−N(5), 92.4(2); P(4)−Ru(2)−N(5), 96.37(18); Ru(2)−N(5)−N(6), 173.6(6).

found for the complex containing dippe, 1.961(3) Å. The Ru(1)−N(1)−N(2) and Ru(2)−N(5)−N(6) angles of 173.7(6) and 175.3(5)° indicate an almost linear Ru−N_2 assembly, and they compare well to the value of 175.8(4)° in the related dippe complex. Dinitrogen distances N(1)−N(2), 1.094(7) Å, and N(5)−N(6), 1.076(8) Å, are in the typical range found in other dinitrogen ruthenium complexes indicating a slight activation of the N_2 ligand. The bond lengths Ru(1)−P(1), 2.2448(17) Å, and Ru(1)−P(2), 2.4148(17) Å, in the first cation, and Ru(2)−P(3), 2.4142(19) Å, and Ru(2)−P(4), 2.2812(18) Å, in the second independent cation, were found nonequivalent in the crystal. A theoretical calculation fully optimizing the geometry of the cation $[(\eta^5\text{-}C_5H_5)Ru(N_2)(R,R\text{-dippach})]^+$ gives an N_2 coordination in agreement with that in the crystal structure (Ru−N = 1.984 Å, N−N = 1.119 Å, and P−Ru−N angles of 88.0 and 92.9°) but with very similar Ru−P bond distances (2.415 and 2.409 Å). Optimizing the structure of the cation with one shorter Ru−P distance, fixed at the crystal value (2.245 Å), gives an energy only 2.7 kcal/mol above the minimum. This energy can be exceeded by the intermolecular interactions in solid state which could be the origin of the difference in the Ru−P bond distances.

Chloride Abstraction under Air. The isolation of dioxygen complexes $[(\eta^5\text{-}C_5H_5)Ru(O_2)(R,R\text{-dippach})][BPh_4]$ (**4a**), $[(\eta^5\text{-}C_5Me_5)Ru(O_2)(R,R\text{-dippach})][BPh_4]$ (**4b**), and $[(\eta^5\text{-}C_5Me_5)Ru(O_2)(dippae)][BPh_4]$ (**4d**) has been possible when chloride abstraction is carried out under air. These complexes have been characterized by elemental analysis and NMR spectroscopy. They are similar to $[(\eta^5\text{-}C_5Me_5)Ru(O_2)(dippe)][BPh_4]$ that we have already reported[43] and can be also formed during the reactions with other small molecules like H_2, N_2, etc. In this manner $[(\eta^5\text{-}C_5Me_5)Ru(O_2)(dippae)][B\{C_6H_3(CF_3)_2\}_4]$ (**4d′**) crystallized from solutions of **3d** even when very small amounts of dioxygen were present. The structure of **4d′** has been determined by X-ray single-crystal diffraction, and a cation drawing is presented in Figure 5.

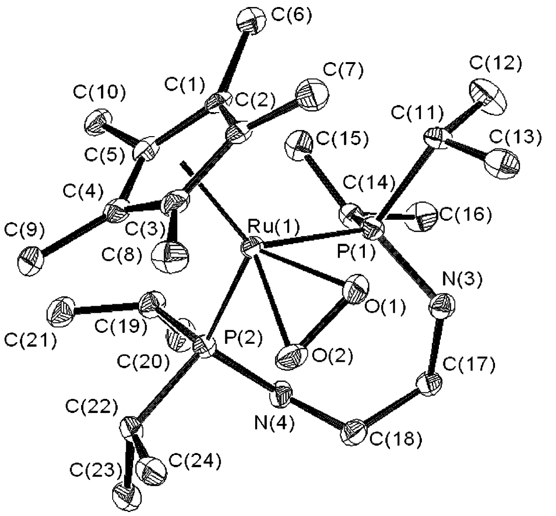

Figure 5. ORTEP drawing (50% thermal ellipsoids) of complex cation $[(\eta^5\text{-}C_5Me_5)Ru(\eta^2\text{-}O_2)(dippae)]^+$ in **4d′**. Hydrogen atoms have been omitted. Selected bond lengths (Å) and angles (deg) with estimated standard deviations in parentheses: Ru(1)−P(1), 2.3972(13); Ru(1)−P(2), 2.3868(16); Ru(1)−O(1), 2.026(3); Ru(1)−O(2), 2.032(3); O(1)−O(2), 1.399(4); P(1)−Ru(1)−P(1), 88.03(5); O(1)−Ru(1)−O(2), 40.33(11); O(1)−O(2)−Ru(1), 69.62(16); O(2)−O(1)−Ru(1), 70.05(16).

The chloride complex $[(\eta^5\text{-}C_5Me_5)RuCl(R,R\text{-dippach})]$ seems to be even more reactive than $[(\eta^5\text{-}C_5Me_5)RuCl(dippae)]$ to trap very small amounts of dioxygen present in solution. On the other hand, the dioxygen complex $[(\eta^5\text{-}C_5H_5)Ru(O_2)(R,R\text{-dippach})][BPh_4]$ (**4a**) represents the first isolated dioxygen complex containing the fragment {CpRu}. In a previous work we have reported the decomposition of the dinitrogen complex $[(\eta^5\text{-}C_5H_5)Ru(N_2)(dippe)][BPh_4]$[43] to the already well-known final product $[(\eta^5\text{-}C_5H_5)Ru(\eta^6\text{-}C_6H_5\text{-}BPh_3)]$. The formation of this sandwich ruthenium complex has been proposed to go through an intermediary dioxygen complex. The complex $[(\eta^5\text{-}C_5H_5)Ru(O_2)(R,R\text{-dippach})][BPh_4]$ (**4a**) is a stable yellow compound in the solid state. Nevertheless, when a solution of **4a** in $CDCl_3$ was followed by NMR during 24 h the dioxygen complex transferring dioxygen to the phosphinoamine ligand or by an alternative mechanism leads also to the sandwich complex $[(\eta^5\text{-}C_5H_5)Ru(\eta^6\text{-}C_6H_5BPh_3)]$.[44] In the presence of $[BAr'_4]^-$ instead of $[BPh_4]^-$ even the poorly coordinative fluorobenzene solvent molecule can been "trapped". Thus, small amounts of the novel sandwich complex $[(\eta^5\text{-}C_5Me_5)Ru(\eta^6\text{-}C_6H_5F)][BAr'_4]$ (**5a**) are obtained in the course of chloride abstraction reactions to obtain dinitrogen or dioxygen complexes. A small fraction of colorless crystals of **5a** was obtained from the solution in which $[(\eta^5\text{-}C_5H_5)Ru(N_2)(R,R\text{-dippach})][BAr'_4]$

---

(43) de los Rios, I.; Jimenez Tenorio, M.; Padilla, J.; Puerta, M. C.; Valerga, P. *J. Chem. Soc., Dalton Trans.* **1996**, 377.

(44) de los Rios, I.; Jimenez Tenorio, M.; Padilla, J.; Puerta, M. C.; Valerga, P. *Organometallics* **1996**, *15*, 4565.

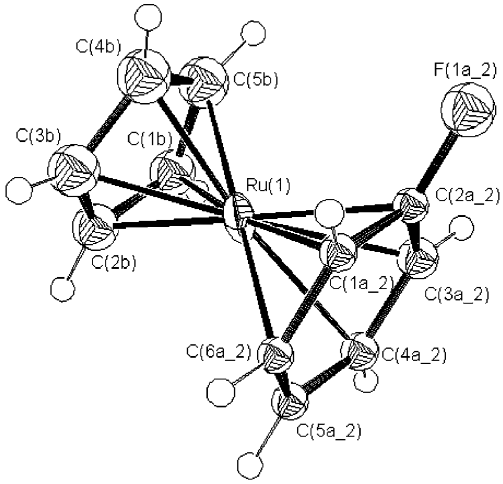

Figure 6. ORTEP drawing (50% thermal ellipsoids) of one cation $[(\eta^5\text{-}C_5Me_5)Ru(FPh)]^+$ in **5a**. Selected bond lengths (Å) with estimated standard deviations in parentheses follow. Cation 1: Ru(1)−C(1b), 2.232(10); Ru(1)−C(2b), 2.194(10); Ru(1)−C(3b), 2.086(10); Ru(1)−C(4b), 2.057(10); Ru(1)−C(5b), 2.150(9); Ru(1)−C(1a_2), 2.148(7); Ru(1)−C(2a_2), 2.191(7); Ru(1)−C(3a_2), 2.274(8); Ru(1)-C(4a_2), 2.316(7); Ru(1)−C(5a_2), 2.276(6); Ru(1)−C(6a_2), 2.192(7); F(1a_2)−C(2a_2), 1.299(10). Cation 2: Ru(2)−C(7a), 2.201(12); Ru(2)−C(8a), 2.151(14); Ru(2)−C(9a), 2.070(12); Ru(2)−C(10a), 2.073(9); Ru(2)−C(11a), 2.154(10); Ru(2)-C(7b_2), 2.183(8); Ru(2)−C(8b_2), 2.214(10); Ru(2)−C(9b_2), 2.282(8); Ru(2)−C(10b_2), 2.318(6); Ru(2)−C(11b_2), 2.288(6); Ru(2)−C(12b_2), 2.220(6); F(2b_2)−C(8b_2), 1.256(11).

(**3a**) was prepared. The structure of **5a** has been determined by X-ray single-crystal diffraction, and a cation drawing is presented in Figure 6. The structure of this Cp sandwich cation is similar to that of its related Cp* complex $[(\eta^5\text{-}C_5Me_5)Ru(\eta^6\text{-}C_6H_5F)]^+$ obtained like a subproduct by chloride abstraction from diphosphine complexes of formula [Cp*RuCl(PP)].[38] Ru−C bond distances are in the normal range obtained for other sandwich or arene complexes of Ru(II).

Conclusion

Novel coordinatively unsaturated ruthenium semisandwich complexes with phosphinoamine ligands and some other related species as dinitrogen and dioxygen complexes are reported. The high reactivity of these 16 electron species is well-known as well as some pathways in which they achieve a relative increase in stability: (1) the formation of dimers or oligomers; (2) the reaction to trap small molecules; (3) the interaction with an agostic H atom in a ligand group, etc. A new way in which the unsaturated species achieve relative stability is now reported. It consists in a mode of coordination not yet described: the chelating phosphinoamine bond to the metal center using three donor atoms and in one side of the chelate ring the metal receiving electron charge simultaneously from a vicinal pair of soft and hard bases (η^2-*P*,*N*). Comparing phosphinoamine ligands dippae and *R*,*R*-dippach, DFT studies have pointed out that a tridentate 18-electron structure is reached because of less destabilization, in the case of *R*,*R*-dippach, by ligand distortion bringing near to the metal a N atom which coordination sufficiently compensates in such case the destabilization energy.

Experimental Section

All synthetic operations were performed under a dry argon atmosphere, using conventional Schlenk techniques. Tetrahydrofuran, diethyl ether, and petroleum ether (boiling point range 40−60 °C) were distilled from the appropriate drying agents. Fluorobenzene was purchased from Aldrich and acetone (0.01% water maximum) from SDS. All solvents were deoxygenated inmediately before use. The complex $\{(\eta^5\text{-}C_5Me_5)RuCl\}_4$[45] as well as $[NaBAr'_4]$[46] was prepared according to reported procedures. The ligands *R*,*R*-dippach and dippae were prepared by following suitable adaptations of published procedures.[23,47,48] IR spectra were recorded in Nujol mulls on a Perkin-Elmer Spectrum 1000 spectrophotometer. NMR spectra were taken on Varian Unity 400 MHz or Varian Gemini 300 MHz equipment using the suitable deuterated solvent. Chemical shifs are given in ppm from $SiMe_4$ (^1H and $^{13}C\{^1H\}$) and 85% H_3PO_4 ($^{31}P\{^1H\}$). Microanalyses were performed on a elemental analyzer model LECO CHNS-932 at the Servicio Central de Ciencia y Tecnología, Universidad de Cádiz.

$[(\eta^5\text{-}C_5H_5)RuCl(R,R\text{-dippach})]$ (1a). To a solution of $[(\eta^5\text{-}C_5H_5)RuCl(PPh_3)_2]$ (3 g, 4.0 mmol) in toluene (20 mL) was added *R*,*R*-dippach (1.6 mL, 4.0 mmol). The mixture was stirred for 2 h under reflux. Then the solvent was removed under vacuum and the residue washed three times with petroleum ether. A microcrystalline orange solid was formed which was dried in vacuo. Yield: 2.2 g, 80%. Anal. Calcd for $C_{23}H_{45}N_2ClP_2Ru$: C, 50.4; H, 8.28; N, 5.11. Found: C, 49.9; H, 8.39; N, 5.55. ^1H NMR (400 MHz, C_6D_6, 298 K): δ 0.92 and 1.22 (m, 24 H, $PCH(CH_3)_2$), 1.46 (m, 8H, (CH_2), 1.86 (m, 2 H, NH), 2.27 (m, 4 H, $PCH(CH_3)_2$), 3.87 (m, 2 H, $(CH)_2(CH_2)_4$), 4.67 (s, 5 H, Cp). $^{31}P\{^1H\}$ NMR (161.89 MHz, C_6D_6, 298 K): δ 112.6 (d, $J_{pp} = 51$ Hz), 113.8 (d, $J_{pp} = 51$ Hz). $^{13}C\{^1H\}$ NMR (75.4 MHz, C_6D_6, 298 K): δ 15.8, 17.1, 18.6, 18.9, 19.5, 19.7, 19.9 and 20.9 (all s, $PCH(CH_3)_2$)), 25.4, 25.8, 27.1 and 28.2 (all s, $(CH_2)_4$), 34.5, 35.9, 36.8 and 37.5 (m, $PCH(CH_3)_2$), 57.8 and 59.8 (s, $(CH)_2(CH_2)_4$), 76.3 (s, Cp).

$[(\eta^5\text{-}C_5Me_5)RuCl(R,R\text{-dippach})]$ (1b). To a solution of $\{(\eta^5\text{-}C_5Me_5)RuCl\}_4$ (1 g, 3.6 mmol) in petroleum ether (20 mL) was added *R*,*R*-dippach (1.5 mL, 3.6 mmol). The mixture was stirred at room temperature for 5 min, and an orange microcrystalline solid precipitated. The solid was filtered out and dried in vacuo. Yield: 1.6 g (72%). Anal. Calcd for $C_{28}H_{55}N_2ClP_2Ru$: C, 54.4; H, 8.97; N 4.53. Found: C, 54.1; H, 8.90; N, 4.25. ^1H NMR (400 MHz, $CDCl_3$, 298 K): δ 1.16 (m, 24 H, $PCH(CH_3)_2$), 1.27 (m, 8H, (CH_2), 1.55(s, 15 H, $C_5(CH_3)_5$), 1.79 (m, 2 H, NH), 2.12 (m, 4 H, $PCH(CH_3)_2$), 2.93 (m, 2 H, $(CH)_2(CH_2)_4$). $^{31}P\{^1H\}$ NMR (161.89 MHz, $CDCl_3$, 298 K): δ 108.3 (d, $J_{pp} = 58$ Hz), 111.7 (d, $J_{pp} = 58$ Hz). $^{13}C\{^1H\}$ NMR (75.4 MHz, $CDCl_3$, 298 K): δ 10.8 (s, $C_5(CH_3)_5$), 18.0, 18.2, 18.3, 19.1, 19.5, 19.9 and 20.0 (all s, $PCH(CH_3)_2$)), 25.2, 25.6, 28.7 and 29.4 (all s, $(CH_2)_4$), 31.4, 34.2, 35.1 and 36.2 (m, $PCH(CH_3)_2$), 57.6 and 60.3 (s, $(CH)_2(CH_2)_4$), 88.1 (s, $C_5(CH_3)_5$).

$[(\eta^5\text{-}C_5H_5)RuCl(\text{dippae})]$ (1c). This compound was obtained in a fashion analogous to that for **1a**, starting from $[(\eta^5\text{-}C_5H_5)RuCl(PPh_3)_2]$ (3 g, 4.0 mmol) and dippae (1.2 mmol). Yield: 1.6 g (80%). Anal. Calcd for $C_{19}H_{39}N_2ClP_2Ru$: C, 46.2; H, 7.96; N, 5.67. Found: C, 45.9; H, 8.10; N, 5.74. ^1H NMR (400 MHz, C_6D_6, 298 K): δ 0.84, 1.07 and 1.41 (m, 24 H, $PCH(CH_3)_2$), 1.98 (m, 2 H, NH), 2.13 and 2.26 (m, 4 H, $PCH(CH_3)_2$), 2.67 and 3.01 (m, 4 H,

---

(45) Tilley, T. D.; Grubbs, R. H.; Bercaw, J. E. *Organometallics* **1984**, *3*, 274.

(46) Brookhart, M.; Grant, B.; Volpe, A. F., Jr. *Organometallics* **1992**, *11*, 3920.

(47) Wiegraebe, W.; Bock, H. *Chem. Ber.* **1968**, *101*, 1414.

(48) Miyano, S.; Nawa, M.; Hashimoto, H. *Chem. Lett.* **1980**, 729.

(CH_2)), 4.60 (s, 5 H, Cp). $^{31}P\{^1H\}$ NMR (161.89 MHz, C_6D_6, 298 K): δ 118.0 (s). $^{13}C\{^1H\}$ NMR (75.4 MHz, C_6D_6, 298 K): δ 17.5, 18.0, 19.1 and 19.8 (m, $PCH(CH_3)_2$)), 31.1 and 31.9 (m, $PCH(CH_3)_2$), 45.8 (s, $(CH_2)_2$), 76.5 (C_5H_5).

[(η^5-C_5Me_5)RuCl(dippae)] (1d). This compound was obtained by following the same procedure used for **1b**, starting from {(η^5-C_5Me_5)RuCl}$_4$ (1 g, 3.6 mmol) and dippae (1.1 mmol). Yield: 1.6 g (80%). Anal. Calcd for $C_{24}H_{49}N_2ClP_2Ru$: C, 51.1; H, 8.75; N, 4.97. Found: C, 51.6; H, 8.91; N, 5.04. ^1H NMR (400 MHz, C_6D_6, 298 K): δ 1.04 (m, 24 H, $PCH(CH_3)_2$), 1.66 ($C_5(CH_3)_5$), 1.70 (m, 2 H, NH), 2.12 (m, 4 H, $PCH(CH_3)_2$), 2.87 and 3.19 (m, 4 H, (CH_2)). $^{31}P\{^1H\}$ NMR (161.89 MHz, C_6D_6, 298 K): δ 111.5 (s). $^{13}C\{^1H\}$ NMR (75.4 MHz, C_6D_6, 298 K): δ 10.8 (s, $C_5(CH_3)_5$), 18.4, 19.0, 19.4 and 19.8 (s, $PCH(CH_3)_2$)), 29.8 (m, $PCH(CH_3)_2$), 46.4 (s, $(CH_2)_2$), 88.5 (C_5H_5).

[(η^5-C_5Me_5)Ru(*R*,*R*-dippach)][BAr′$_4$] (2b). To a solution of **1b** (0.6 g, 1 mmol) in fluorobenzene (12 mL) under argon was added NaBAr′$_4$ (0.9 g, 1 mmol). The mixture was stirred at room temperature for 10 min. Sodium chloride was removed by filtration through Celite. The filtrate was concentrated to obtain a microcrystaline orange solid. Yield: 0.40 g (40%). Anal. Calcd for $C_{60}H_{67}N_2P_2F_{24}BRu$: C, 49.2; H, 4.65; N, 3.70. Found C, 49.3; H, 4.57; N, 3.85. ^1H NMR (400 MHz, CD_2Cl_2, 298 K): δ 1.17 (m, 32 H, $PCH(CH_3)_2$, (CH_2)), 1.70 (s, 15 H, $C_5(CH_3)_5$), 1.82 (m, 2 H, NH), 2.07 (m, 4 H, $PCH(CH_3)_2$), 3.22 (m, 2 H, $(CH)_2(CH_2)_4$). $^{31}P\{^1H\}$ NMR (161.89 MHz, CD_2Cl_2, 298 K): δ 92.3 (s). $^{13}C\{^1H\}$ NMR (75.4 MHz, CD_2Cl_2, 298 K): δ 10.8 (s, $C_5(CH_3)_5$), 18.1, 18.3, 19.1, 19.3, 19.4, 19.5, 19.8 and 20.0 (s, $PCH(CH_3)_2$)), 25.2, 25.6, 28.7 and 32.2 and 35.6 (s, $(CH_2)_4$), 35.1 and 36.2 (m, $PCH(CH_3)_2$), 57.7 and 60.3 (s, $(CH)_2(CH_2)_4$), 88.1 (s, $C_5(CH_3)_5$).

[(η^5-C_5Me_5)Ru(dippae)][BAr′$_4$] (2d). To a solution of **1d** (0.6 g, 1 mmol) in fluorobenzene (12 mL) under argon was added NaBAr′$_4$ (0.9 g, 1 mmol). The mixture was stirred for 5 min, and a change color from orange to dark blue was observed. The solution was filtered through Celite, and the filtrate was concentrated under reduced pressure to a volume of ca. 1 mL and then layered with petroleum ether and left undisturbed at room temperature. Blue crystals were obtained by slow diffusion of petroleum ether into the fluorobenzene. The crystals were separated from the supernatant liquor, washed with petroleum ether, and dried in an argon stream. Yield: 0.42 g (50%). Anal. Calcd for $C_{56}H_{61}N_2F_{24}P_2BRu$: C, 47.6; H, 4.43; N, 2.88. Found: C, 47.9; H, 4.47; N, 2.84. ^1H NMR (400 MHz, CD_2Cl_2, 298 K): δ 1.10, 1.26 and 1.37 (m, 24 H, $PCH(CH_3)_2$), 1.59 ($C_5(CH_3)_5$), 2.34 and 2.48 (m, 4 H, $PCH(CH_3)_2$), 2.79 and 3.11 (m, 4 H, (CH_2)), NH hydrogens not observed. $^{31}P\{^1H\}$ NMR (161.89 MHz, CD_2Cl_2, 298 K): δ 96.4 (s). $^{13}C\{^1H\}$ NMR (75.4 MHz, CD_2Cl_2, 298 K): δ 11.8 s, $C_5(CH_3)_5$), 14.4, 14.7, 15.7, 19.8, 21.1 and 23.1 (s, $PCH(CH_3)_2$)), 30.8 and 34.9 (m, $PCH(CH_3)_2$), 42.1 (s, $(CH_2)_2$), 66.3 ($C_5(CH_3)_5$).

[(η^5-C_5H_5)Ru(N_2)(*R*,*R*-dippach)][BAr′$_4$] (3a). To a solution of **1a** (0.6 g, 1 mmol) in fluorobenzene (12 mL) under a N_2 atmosphere was added solid NaBAr′$_4$ (0.9 g, 1 mmol). The mixture was stirred for minutes at room temperature. Sodium chloride was removed by filtration through Celite. After concentration of the resulting solution to a volume of ca. 1 mL, petroleum ether was added and the resulting solution was left undisturbed at room temperature. A microcrystalline yellow solid was formed, which was separated from the supernatant liquor, washed with petroleum ether, and dried in vacuo. Yield: 0.71 g (60%). Anal. Calcd for $C_{55}H_{57}N_4P_2F_{24}BRu$: C, 47.1; H, 4.09; N, 3.99. Found: C, 47.6; H, 4.25; N, 3.86. IR (Nujol): ν (N_2) 2186 (s) cm^{-1}. ^1H NMR (400 MHz, CD_2Cl_2, 298 K): δ 1.19 (m, 32 H, $PCH(CH_3)_2$, (CH_2)), 1.82 (m, 2 H, NH), 2.29 (m, 4 H, $PCH(CH_3)_2$), 2.84 (m, 2 H, $(CH)_2(CH_2)_4$), 5.14 (s, 5 H, Cp). $^{31}P\{^1H\}$ NMR (161.89 MHz, CD_2Cl_2, 298 K): δ 110.6 (d, $^2J_{PP}$ = 39 Hz), 112.5 (d, $^2J_{PP}$ = 39 Hz). $^{13}C\{^1H\}$ NMR (75.4 MHz, CD_2Cl_2, 298 K): δ 16.1, 16.3, 17.4, 18.2, 18.8 and 19.7 (all s, $PCH(CH_3)_2$)), 24.6 and 25.3 (all s, $(CH_2)_4$), 34.8 and 35.8 (m, $PCH(CH_3)_2$), 58.0 and 59.8 (s, $(CH)_2(CH_2)_4$), 81.8 (s, Cp).

[(η^5-C_5Me_5)Ru(N_2)(*R*,*R*-dippach)][BAr′$_4$] (3b). This compound was obtained by following the same procedure used for of **3a**, starting from **1b** (0.6 g, 1 mmol). Yield: 0.52 g (40%). Anal. Calcd for $C_{60}H_{67}N_4P_2F_{24}BRu$: C, 48.9; H, 4.58; N, 3.80. Found: C, 49; H, 4.25; N, 3.96. IR (Nujol): ν (N_2) 2142 (s) cm^{-1}. ^1H NMR (400 MHz, CD_2Cl_2, 298 K): δ 1.17 (m, 32 H, $PCH(CH_3)_2$, (CH_2)), 1.70 (s, 15 H, $C_5(CH_3)_5$), 1.82 (m, 2 H, NH), 2.07 (m, 4 H, $PCH(CH_3)_2$), 3.22 (m, 2 H, $(CH)_2(CH_2)_4$). $^{31}P\{^1H\}$ NMR (161.89 MHz, CD_2Cl_2, 298 K): δ 99.7 (d, $^2J_{PP}$ = 47 Hz) and 102.0 (d, $^2J_{PP}$ = 47 Hz).

[(η^5-C_5H_5)Ru(N_2)(dippae)][BAr′$_4$] (3c). This compound was obtained by following the same procedure used for of **3a**, starting from **1c** (0.6 g, 1 mmol). Yield: 1.6 g (80%). Anal. Calcd for: $C_{51}H_{51}N_4P_2F_{24}BRu$: C, 45.4; H, 3.81; N, 4.15. Found: C, 45.3; H, 3.90; N, 4.25. IR (Nujol): ν (N_2) 2178 (s) cm^{-1}. ^1H NMR (400 MHz, CD_2Cl_2, 298 K): δ 1.05 and 1.25 (m, 24 H, $PCH(CH_3)_2$), 1.65 (m, 2 H, NH), 2.08 and 2.13 (m, 4 H, $PCH(CH_3)_2$), 2.98 and 3.21 (m, 4 H, (CH_2)), 4.75 (s, 5 H, Cp). $^{31}P\{^1H\}$ NMR (161.89 MHz, CD_2Cl_2, 298 K): δ 99.1 (s). $^{13}C\{^1H\}$ NMR (75.4 MHz, CD_2Cl_2, 298 K): δ 18.2, 18.5, 19.1 and 19.7 (m, $PCH(CH_3)_2$)), 32.1 and 32.9 (m, $PCH(CH_3)_2$), 46.2 (s, $(CH_2)_2$), 76.9 (C_5H_5).

[(η^5-C_5Me_5)Ru(N_2)(dippae)][BAr′$_4$] (3d). This compound was obtained by following the same procedure used for of **3a**, starting from **1d** (0.6 g, 1 mmol). Yield: 0.42 g (50%). Anal. Calcd for $C_{56}H_{61}N_4F_{24}P_2BRu$: C, 47.4; H, 4.33; N, 3.95. Found: C, 47.6; H, 3.39; N, 3.84. IR (Nujol): ν (N_2) 2201 (s) cm^{-1}. ^1H NMR (400 MHz, CD_2Cl_2, 298 K): δ 1.15 (m, 24 H, $PCH(CH_3)_2$), 1.69 ($C_5(CH_3)_5$), 1.70 (m, 2 H, NH), 2.35 (m, 4 H, $PCH(CH_3)_2$), 2.80 and 3.08 (m, 4 H, (CH_2)). $^{31}P\{^1H\}$ NMR (161.89 MHz, CD_2Cl_2, 298 K): δ 92.6(s). $^{13}C\{^1H\}$ NMR (75.4 MHz, CD_2Cl_2, 298 K): δ 10.2 s, $C_5(CH_3)_5$), 19.1, 19.2, 19.4 and 19.9 (s, $PCH(CH_3)_2$)), 30.2 (m, $PCH(CH_3)_2$), 47.6 (s, $(CH_2)_2$), 90.2 ($C_5(CH_3)_5$).

[(η^5-C_5H_5)Ru(O_2)(*R*,*R*-dippach)][BPh$_4$] (4a). Complex **1a** (0,6 g, 1 mmol) was dissolved in MeOH in the air. Addition of an excess of solid NaBPh$_4$ (0.5 g) produced a yellow precipitate, which was filtered out, washed with ethanol and light petroleum, and dried in vacuo. Yield: 0.30 g (35%). Anal. Calcd for $C_{47}H_{65}N_2O_2P_2BRu$: C, 65.3; H, 7.58; N, 3.24. Found: C, 65.4; H, 7.69; N, 3.17. ^1H NMR (400 MHz, $CDCl_3$, 298 K): δ 1.28 (m, 32 H, $PCH(CH_3)_2$, (CH_2)), 1.90 (m, 2 H, NH), 2.17 and 2.69 (m, 4 H, $PCH(CH_3)_2$), 3.14 (m, 2 H, $(CH)_2(CH_2)_4$), 5.33 (s, 5 H, Cp). $^{31}P\{^1H\}$ NMR (161.89 MHz, $CDCl_3$, 298 K): δ 103.0 (d, $^2J_{PP}$ = 35 Hz), 104.4 (d, $^2J_{PP}$ = 35 Hz). $^{13}C\{^1H\}$ NMR (75.4 MHz, CD_2Cl_2, 298 K): δ 16.1, 16.3, 17.4, 18.2, 18.8 and 19.7 (all s, $PCH(CH_3)_2$)), 24.6 and 25.3 (all s, $(CH_2)_4$), 34.8 and 35.8 (m, $PCH(CH_3)_2$), 58.0 and 59.8 (s, $(CH)_2(CH_2)_4$), 81.8 (s, Cp).

[(η^5-C_5Me_5)Ru(O_2)(*R*,*R*-dippach)][BPh$_4$] (4b). This compound was obtained by following the same procedure used for of **4a**, starting from **1b** (0.6 g, 1 mmol). Yield: 0.52 g (40%). Anal. Calcd for $C_{52}H_{75}N_2O_2P_2BRu$: C, 66.8; H, 8.09; N, 3.00. Found: C, 66.9; H, 8.16; N, 3.10. ^1H NMR (400 MHz, $CDCl_3$, 298 K): δ 0.98, 1.18 and 1.35 (m, 32 H, $PCH(CH_3)_2$, (CH_2)), 1.52 (s, 15 H, $C_5(CH_3)_5$), 2.15 (m, 2 H, NH), 1.99 and 2.30 (m, 4 H, $PCH(CH_3)_2$), 2.79 and (m, 2 H, $(CH)_2(CH_2)_4$). $^{31}P\{^1H\}$ NMR (161.89 MHz, $CDCl_3$, 298 K): 86.2 (d, $^2J_{PP}$ = 47.5 Hz), 94.4 (d, $^2J_{PP}$ = 47.5 Hz). $^{13}C\{^1H\}$ NMR (75.4 MHz, $CDCl_3$, 298 K): δ 10.5 (s, $C_5(CH_3)_5$), 15.9, 18.7, 19.4 and 20.2 (m, $PCH(CH_3)_2$)), 24.4, 26.5, 29.0 and 32.7 (all d, $^2J_{CP}$ = 27 Hz, $(CH_2)_4$), 34.7 and 35.8 (m, $PCH(CH_3)_2$), 57.5 and 60.2 (s, $(CH)_2(CH_2)_4$), 106.2 (s, $C_5(CH_3)_5$).

[(η^5-C$_5$Me$_5$)Ru(O$_2$)(dippae)][BPh$_4$] (4d). This compound was obtained by following the same procedure used for of **4a**, starting from **1d** (0.6 g, 1 mmol). Yield: 0.42 g (50%). Anal. Calcd for: C$_{44}$H$_{69}$N$_2$O$_2$P$_2$BRu: C, 63.5; H, 8.36; N, 3.37. Found: C, 63.5; H, 8.39; N, 3.84. ^{1}H NMR (400 MHz, CDCl$_3$, 298 K): δ 1.15−1.32 (m, 24 H, PCH(CH_3)$_2$), 1.51 (C$_5$(CH_3)$_5$), 1.74 (m, 2 H, NH), 2.33 (m, 4 H, PCH(CH$_3$)$_2$), 2.55 and 2.83 (m, 4 H, (CH_2)). ^{31}P{^{1}H} NMR (161.89 MHz, CDCl$_3$, 298 K): δ 87.2 (s). ^{13}C{^{1}H} NMR (75.4 MHz, CDCl$_2$, 298 K): δ 10.3 s, C$_5$(CH$_3$)$_5$), 17.6, 18.8 and 19.3 (s, PCH(CH$_3$)$_2$)), 31.4 (m, PCH(CH$_3$)$_2$), 45.3 (s, (CH$_2$)$_2$), 100.7 (C_5(CH$_3$)$_5$).

[(η^5-C$_5$Me$_5$)Ru(η^2-O$_2$)(dippae)][BAr′$_4$] (4d′). This compound was obtained by following the same procedure used for of **4a**, starting from **1d** (0.6 g, 1 mmol). Yield: 1.18 g (83%). Anal. Calcd for: C$_{56}$H$_{61}$N$_2$F$_{24}$O$_2$P$_2$BRu: C, 47.2; H, 4.28; N, 1.97. Found: C, 47.6; H, 4.35; N, 1.8. IR: ν(NH) 33340−3345 cm^{-1}. ^{1}H NMR (400 MHz, CDCl$_3$, 298 K): δ 1.15−1.35 (m, 24 H, PCH(CH_3)$_2$), 1.54 (s, 15H, C$_5$(CH_3)$_5$), 1.75 (m, 2 H, NH), 2.35 (m, 4 H, PCH(CH$_3$)$_2$), 2.57 and 2.80 (m, 4 H, (CH_2)), 7.48−7.6 (m, 12 H, C$_6$$H_3$(CF$_3$)$_2$. ^{31}P{^{1}H} NMR (161.89 MHz, CDCl$_3$, 298 K): δ 88.2 (s). ^{13}C{^{1}H} NMR (75.4 MHz, CDCl$_2$, 298 K): δ 10.9 s, C$_5$(CH$_3$)$_5$), 17.9, 19.0, 19.4 and 19.9 (s, PCH(CH$_3$)$_2$)), 32.1 (m, PCH(CH$_3$)$_2$), 46.0 (s, (CH$_2$)$_2$), 102.5 (C_5(CH$_3$)$_5$), 116.7 (s, C$_{para}$ of Ar′), 123.9 (q, $^1J_{CF} = 270$ Hz, CF$_3$ of Ar′), 128.0 (m, C$_{meta}$ of Ar′), 134.0 (s, C$_{ortho}$ of Ar′), 160.9 (q, $^1J_{BC} = 49$ Hz, C$_{ipso}$ of Ar′).

[Ru(η^5-C$_5$H$_5$)(η^6-C$_6$H$_5$F)][BAr′$_4$] (5a). From solutions of dinitrogen complex **3a** or dioxygen complex **4a** in fluorobenzene, the presence of 16 electron [(η^5-C$_5$H$_5$)Ru(*R*,*R*-dippach)]$^+$ produced the coordination of the solvent and a small fraction of colorless crystals of [Ru(η^5-C$_5$H$_5$)(η^6-C$_6$H$_5$F)][BAr′$_4$] was obtained. Anal. Calcd for C$_{43}$H$_{22}$F$_{25}$BRu: C, 50.4; H, 2.16. Found: C, 50.3; H, 2.30. ^{1}H NMR (400 MHz, CDCl$_3$, 298 K): δ 4.68 (s, 5 H, Cp), 5.56, 6.15 (bs, 5 H, C$_6$$H_5$F), 7.48−7.6 (m, 12 H, {C$_6$$H_3$(CF$_3$)$_2$}$_4$). ^{13}C{^{1}H} NMR (75.4 MHz, CD$_2$Cl$_2$, 298 K): δ 16.1, 16.3, 17.4, 18.2, 18.8 and 19.7 (all s, PCH(CH$_3$)$_2$)), 24.6 and 25.3 (all s, (CH$_2$)$_4$), 34.8 and 35.8 (m, PCH(CH$_3$)$_2$), 58.0 and 59.8 (s, (CH)$_2$(CH$_2$)$_4$), 81.8 (s, Cp).

X-ray Structure Determinations. Suitable crystals for X-ray diffraction analysis were obtained for compounds **2b**, **3a**, **5a**, and **4d′**. In each case a single crystal was mounted on a glass fiber to carry out the crystallographic study. Crystal data and experimental details are given in Table 2. X-ray diffraction data collections were measured at 100 K on a Bruker Smart APEX CCD 3-circle diffractometer using a sealed tube source, graphite-monochromated Mo Kα radiation ($\lambda = 0.710\,73$ Å), at the Servicio Central de Ciencia y Tecnología de la Universidad de Cádiz. Diffraction data were recorded in four sets of frames over a hemisphere of the reciprocal space by ω scan with $\delta(\omega)$ 0.30° and exposure of 10 s/frame. Correction for absorption and crystal decay (insignificant) were applied by semiempirical method from equivalents using program SADABS.[49] The structures were solved by direct methods, completed by subsequent difference Fourier syntheses, and refined on F^2 by full-matrix least-squares procedures using the programs contained in SHELXTL package.[50] Most of non-hydrogen atoms were refined with anisotropic displacement parameters. For **2b** and **5a** some of the F atoms in CF$_3$ groups were disordered over two positions. Only the part with sof > 0.5 was refined anisotropically Additionally, in the case of **5a** the cation was found disordered in two positions. In both of them half of the occupation was attributed to η^5-C$_5$H$_5$ and half to η^6-C$_6$H$_5$F (fluorobenzene). These C and F atoms were isotropically refined. The hydrogen atoms were refined using the SHELX riding model. The program ORTEP-3[51] was used for plotting. CCDC 605986−605988 files giving crystallographic data for **2b**, **3a**, and **5a** and CCDC 638106 for **4d′** are available free of charge via Internet at http://www.ccdc.cam.ac.uk/conts/retrieving.html or as Supporting Information at http://pubs.acs.org.

Computational Details. The calculations have been performed using the Gaussian03 package.[52] The geometries have been fully optimized using density functional theory with the B3LYP functional.[53−55] For the Ru and P atoms, the lanl2dz effective core potential has been used to describe the inner electrons,[52,56,57] whereas their associated double-ζ basis set has been employed for the remaining electrons. An extra series of d-polarization functions has also been added for P (expt 0.387).[58] For all the carbon and nitrogen atoms the 6-31G(d) basis set has been used. H atoms have been described by the 6-31G basis set.[59−61]

Acknowledgment. We thank the Spanish Ministerio de Educación y Ciencia (Projects CTQ2004-00776/BQU and CTQ2005-09000-CO2-01 and Grant BES2002-1422 to M.D.P.) and Junta de Andalucia (Group PAI FQM188 and Project PAI05 FQM00094) for financial support, Johnson Matthey plc for generous loans of ruthenium trichloride, and L. M. Rodriguez Jaren for his help in X-ray data collection. E.V. acknowledges the European Commission through the HYDROCHEM program (Contract HPRN-CT-2002-00176). The use of the computational facilities at the Centre de Supercomputació de Catalunya (CESCA) is appreciated as well.

Supporting Information Available: Complete ref 52 and Cartesian coordinates and absolute energies for the optimized structures. This material is available free of charge via the Internet at http://pubs.acs.org

IC700674C

---

(49) Sheldrick, G. M. *SADABS*, 2001 version; University of Göttingen: Göttingen, Germany, 2001.

(50) *SHELXTL*, v. 6.10; Bruker-AXS: Madison, WI, 2000. Sheldrick, G. M. *SHELXS-86 and SHELXL-97*; University of Göttingen: Göttingen, Germany, 1997.

(51) Faruggia, L. J. ORTEP-3 for Windows, version 1.08. *J. Appl. Crystallogr.* **1997**, *30*, 565.

(52) Frisch, M. J.; et al. *Gaussian 03*; Gaussian, Inc.: Wallingford, CT, 2004.

(53) Lee, C.; G.; Yang, W.; Parr, R. *Phys. Rev.* **1988**, *37*, B785.

(54) Becke, A. D. *J. Phys. Chem.* **1993**, *98*, 5648.

(55) Stephens, P. J.; Devlin, F. J.; Chabalowski, C. F.; Frisch, M. J. *J. Phys. Chem.* **1994**, *98*, 11623.

(56) Hay, P. J.; Wadt, W. R. *J. Phys. Chem.* **1985**, *82*, 299.

(57) Wadt, W. R.; Hay, P. J. *J. Phys. Chem.* **1985**, *82*, 284.

(58) Höllwarth, A.; Böhme, M.; Dapprich, S.; Ehlers, A. W.; Gobbi, A.; Jonas, V.; Köhler, K. F.; Stegmann, R.; Veldkamp, A.; Frenking, G. *Chem. Phys. Lett.* **1993**, *208*, 237.

(59) Hehre, W. J.; Ditchfield, R.; Pople, J. A. *J. Phys. Chem. A* **1972**, *56*, 2257.

(60) Hariharan, P. C.; Pople, J. A. *Theor. Chim. Acta* **1973**, *28*, 213.

(61) Francl, M. M.; Pietro, W. J.; Hehre, W. J.; Binkley, J. S.; Gordon, M. S.; DeFrees, D. J.; Pople, J. A. *J. Chem. Phys.* **1982**, *77*, 3654.